Available online at www.sciencedirect.com
SCIENCE DIRECT®
Pattern Recognition Letters 27 (2006) 1361–1369
Pattern Recognition Letters
www.elsevier.com/locate/patrec

Image reconstruction from a complete set of similarity invariants extracted from complex moments

F. Ghorbel [a], S. Derrode [b,*], R. Mezhoud [a], T. Bannour [a], S. Dhahbi [a]

[a] *Laboratoire Cristal, GRIFT, École Nationale des Sciences de l'Informatique, Campus Universitaire de la Manouba, 2010 Manouba, Tunisia*
[b] *Université Paul Cézanne, Institut Fresnel, CNRS UMR 6133, École Généraliste d'Ingénieurs de Marseille, Dom. Universitaire de Saint Jérôme, 13013 Marseille, Cedex 20, France*

Received 4 July 2005; received in revised form 25 November 2005
Available online 9 March 2006

Communicated by Prof. L. Younes

Abstract

Various types of moments have been used to recognize image patterns in a number of applications. However, only few works have paid attention to the completeness property of the invariant descriptor set, which is of fundamental importance from the theoretical as well as the practical points of views. This paper proposes a systematic method to extract a complete set of similarity invariants (translation, rotation and scale), by means of some linear combinations of complex moments. The problem of image reconstruction from a finite set of its moment invariants is then examined by exploiting the link between the discrete Fourier transform of an image and its complex moments. Experimental results are presented that confirm theoretical properties as well as numerical effectiveness of the method.

Keywords: Pattern recognition; Complex moments; Reconstruction; Similarity invariants; Completeness

1. Introduction

Geometric and complex moments are ones of the most common tools for the construction of object descriptors for pattern recognition, target identification and scene analysis. The pioneering works by Ming-Kuel (1962), Davis (1977) have been extended to a variety of new moments, especially orthogonal polynomial moments: Zernike (Khotanzad and Hong, 1990) and Fourier–Merlin (Sheng and Shen, 1994) moments, and more recently, Tchebichev (Mukundan et al., 2001), Krawtchouk (Yap et al., 2003) and radial harmonic Fourier (Ren et al., 2003) moments. The orthogonality property insures that the information coded in the descriptors is not redundant, which is generally considered as an advantage over non orthogonal moments. It is however well known that information redundancy can be of practical interest, especially when images are noisy.

The most important properties to be verified by those descriptors are (i) invariance against some geometrical transformations (translation, rotation, scaling, stretching, etc.), (ii) stability to noise, to blur, to non rigid and small local deformations and (iii) completeness. While the two first properties are commonly studied, less attention has been paid to the third one. A set of invariant descriptors is said to be complete if it encodes all the information on the shape of an object, i.e. everything except the geometrical information characterizing the pose of the object in the image. The first significant work on completeness was due to Crimmins (1982) who derived a complete set of Fourier-based invariant descriptors from object contour. A complete set of similarity (translation, rotation and scale) invariant descriptors computed from the Fourier–Merlin transform has been proposed in (Ghorbel, 1994; Derrode and Ghorbel, 2001).

* Corresponding author. Tel.: +33 4 9128 2849; fax: +33 4 9128 8813.
E-mail addresses: stephane.derrode@egim-mrs.fr, stephane.derrode@fresnel.fr, derrode@egim-mrs.fr (S. Derrode).

0167-8655/$ - see front matter © 2006 Elsevier B.V. All rights reserved.
doi:10.1016/j.patrec.2006.01.001

Regarding moment invariants, the seven descriptors proposed by Ming-Kuel (1962) and the extended sets latter proposed in (Wong et al., 1995; Balslev, 1998), do not achieve completeness. More recently, complex moments have received a renew of interest, notably from works by Flusser and co-workers, with several extensions of classical similarity invariance (Abu-Mostafa and Psaltis, 1984, 1985) to blur (Flusser et al., 1996; Liu and Zhang, 2005), affine (Suk and Flusser, 2003, 2004) and projective (Suk and Flusser, 2004) transformations. They also proposed a complete and independent set of rotation invariants by normalizing complex moments (Flusser, 2002; Flusser and Suk, 2003), which appears to be a particular case of a more general class of complete similarity invariant families introduced earlier in (Derrode et al., 2000) (see Section 2). This family is constructed in a systematic way by using a normalization method inspired by the relation that links complex moments of two objects with the same shape but distinct orientation and scale. Numerical behavior and performance of the set are compared to Mukundan's and Flusser's families of rotation invariants (Mukundan, 2004; Flusser and Suk, 2003) and to Hu's set of similarity invariants, in Section 3.

The inverse problem of complex moments is examined in Section 4, i.e., how it is possible to reconstruct an image from a finite set of its complex moments. The new approach we propose consists in constructing the discrete fourier transform (DFT) of an image from its complex moments and then applying the inverse DFT to recover the original image. We next present some reconstruction experiments showing the practicality of the method and how well an image can be characterized by a small set of its complex moments. Finally, Section 5 summarizes the most important results and mentions future works.

2. A complete set of similarity invariants from complex moments

For an integrable function $f(x,y)$, complex moments can be defined by

$$c_f(p,q) = \int\int_{\mathbb{R}^2} (x+\mathrm{i}y)^p (x-\mathrm{i}y)^q f(x,y)\,\mathrm{d}x\,\mathrm{d}y, \tag{1}$$

where p, $q \in \mathbb{N}$. In polar coordinates, Eq. (1) becomes

$$c_f(p,q) = \int_0^{\infty}\int_0^{2\pi} r^{p+q+1} \mathrm{e}^{\mathrm{i}(p-q)\theta} f(r,\theta)\,\mathrm{d}r\,\mathrm{d}\theta. \tag{2}$$

The origin of the coordinate system is taken at the center of mass of the objects in order to achieve translation invariance of the representation. This center of mass is classically computed from the firsts geometric moments of the object.

It is easy to verify that the relation between complex moments of two images f and g having the same shape but distinct orientation (β) and scale (α), i.e., $g(r,\theta) = f(\alpha r, \theta+\beta)$, is given by

$$\forall p,q \in \mathbb{N}, \quad c_g(p,q) = \alpha^{-(p+q+2)} \mathrm{e}^{-\mathrm{i}(p-q)\beta} c_f(p,q). \tag{3}$$

From (2), Flusser (2002), Flusser and Suk (2003) derived a complete and independent set of rotation invariants (Φ_f) given by

$$\forall p,q \in \mathbb{N}, \quad \Phi_f(p,q) = c_f(p_0-1,p_0)^{p-q} c_f(p,q), \tag{4}$$

where $p_0 > 0$ is an arbitrary index and $c_f(p_0-1,p_0) \neq 0$ acts as a normalization factor to make the complex moments invariant to rotation.

Earlier, Derrode et al. (2000) proposed a complete set of both rotation and scale invariants (I_f), given by

$$\forall p,q \in \mathbb{N}, \quad I_f(p,q) = \Gamma_f^{-(p+q+2)} \mathrm{e}^{-\mathrm{i}(p-q)\Theta_f} c_f(p,q), \tag{5}$$

with $\Theta_f = \arg(c_f(1,0))$ and $\Gamma_f = \sqrt{c_f(0,0)}$.

Coefficients Γ_f and Θ_f normalize independently the magnitude and the phase of complex moments. It is easy to verify that other normalization factors can be used if, for $g(r,\theta) = f(\alpha r, \theta+\beta)$, we get

$$\Theta_f - \Theta_g = \beta(2\pi), \quad \text{and} \quad \frac{\Gamma_f}{\Gamma_g} = \alpha. \tag{6}$$

For example, if we introduce

$$\Theta_f = -\arg(c_f(p_0-1,p_0)), \quad \text{and} \quad \Gamma_f = \sqrt[2(p_1+1)]{|c_f(p_1,p_1)|},$$

in Eq. (5), with $p_0 > 0$ and $p_1 \geqslant 0$, we get another complete family of invariants. Hence, Flusser's complete set of invariants appears as a particular case, with invariance only to rotation since the normalization of magnitude does not make the family invariant to scale transformations.

It is easy to verify that sets of the form (5) are complete since

$$\forall p,q \in \mathbb{N}, \quad c_f(p,q) = \Gamma_f^{p+q+2} \mathrm{e}^{\mathrm{i}(p-q)\Theta_f} I_f(p,q). \tag{7}$$

Hence, if one knows all invariants $I_f(p,q)$ and the two normalization factors Γ_f, Θ_f, it becomes possible to reconstruct back all complex moments $c_f(p,q)$. The question of how it is possible to reconstruct back the original image from its complex moments is addressed in Section 4.

All families of the form (5) with conditions (6) are theoretically equivalent. The choice for the normalization factors should be driven by numerical considerations such as robustness to noise and numerical stability. Generally, factors using small order moments are preferred due to their weak sensitivity to numerical approximation. Experiments presented in next section are performed with the original family (Derrode et al., 2000).

3. Numerical experiments

This section is intended to test the complete family of similarity invariants in Eq. (5) using Lena image in Fig. 1. The set is compared to Hu's similarity invariants (Appendix A), Flusser's complex moment family (Eq. (4)) and Mukundan's radial Tchebichef moment family (Mukundan, 2004) (Eq. (8)) of rotation invariants.

Fig. 1. Lena image, size 200×200.

Rotational invariants can be obtained by taking the magnitude of radial Tchebichef moments according to

$$S_f(p,q) = \frac{1}{n\rho(p,m)} \sum_{r=0}^{m-1} \sum_{\theta=0}^{n-1} t_p(r) \mathrm{e}^{-jq\theta} f(r,\theta), \tag{8}$$

where the image size is $N \times N$, $m = (N/2) + 1$ and n denotes the number of angular sampling points. Also $t_n(r)$ denotes Tchebichef polynomials which satisfy the following recurrence formula

$$(n+1)t_{n+1}(r) - (2n+1)(2r - N + 1)t_n(r) + n\left(1 - \frac{n^2}{N^2}\right)t_{n-1}(r) = 0,$$

with the initial conditions $t_0(r) = 1$ and $t_1(r) = (2r - N + 1)/N$. The squared-norm $\rho(p,m)$ is given by

$$\rho(p,m) = \frac{m}{2p+1} \prod_{i=1}^{p} \left(1 - \left(\frac{i}{m}\right)^2\right), \quad p = 0, \ldots, m-1.$$

The set $\{|S_f(p,q)|\}_{p,q\in\mathbb{N}}$ is not complete since the phase of each moment $S_f(p,q)$ is not taken into account.

To make comparisons possible between all families of invariants, we constructed a 1D vector from a 2D array of invariants by using a zigzag scan starting with order $(p = 0,\ q = 0) \to k = 0$ and following the path $(1,0) \to 1$, $(0,1) \to 2$, $(2,0) \to 3$, $(1,1) \to 4$, $(0,2) \to 5$, etc. The comparison is performed according to the relative error between the invariant vector I_1 from the original image and the invariant vector I_2 from the transformed image:

$$E_{I_1,I_2}(k) = \left|\frac{I_1(k) - I_2(k)}{I_1(k)}\right|. \tag{9}$$

The term $I_1(k)$ in the denominator normalizes the invariants of the four families to the same dynamic range and makes the comparison between the different types of moments possible.

3.1. Invariance to rotation

To test invariance against rotation, we have rotated the Lena image in Fig. 1 by 30°, 60°, 90° and 95°, as shown in Fig. 2. Plots in Fig. 3 compare the relative errors between the invariant vector of the original image and the invariant vectors of the rotated images. Plots clearly show that the relative error is much more higher in the case of Flusser's and Mukundan's families of invariants than in the case of the new set of similarity invariants, whatever the rotation angle. Also, one important point to note is the smooth behavior of the relative errors when computed for the complete set of invariants, compared to others families.

3.2. Invariance to scale

To test invariance against dilatation, we have scaled the Lena image by 85%, 90%, 110% and 125%, as shown in Fig. 4. Plots in Fig. 5 compare the relative errors between the invariant vector of the original image and the invariant vectors of the scaled images, for the complete family and Hu' set of similarity invariants (see Appendix A). If the relative errors are very close for 110% and 125% dilatations, they are higher for Hu' set in the case of 85% and 95% dilatations. This result confirms the robustness of the set to numerical approximations. In addition, one great advantage of the new set against Hu's invariants is the possibility to use as many invariant descriptors as needed for a given pattern recognition application.

3.3. Robustness against noise

To test the robustness of the family against noise, we have added to the Lena image a white Gaussian noise with mean $\mu = 0$ and variance $\sigma^2 = 13$, 20, 28 and 34, as shown in Fig. 6. Plots in Fig. 7 compare the relative errors between the invariant vector of the original image and the invariant vectors of the noisy images. It can be seen that there is no fundamental differences between all the families and, as expected, that higher-order moments are more sensitive to noise. One can however note that the draws

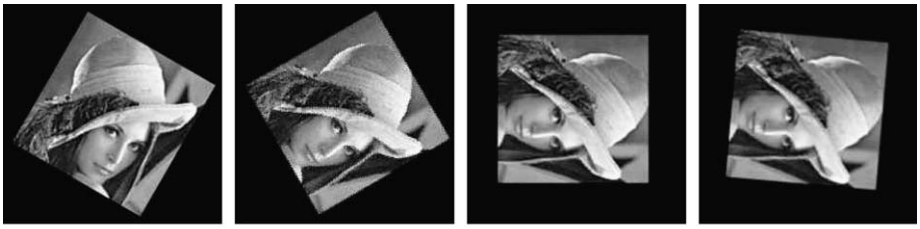

(a) 30° (b) 60° (c) 90° (d) 95°

Fig. 2. Several rotations of the original image.

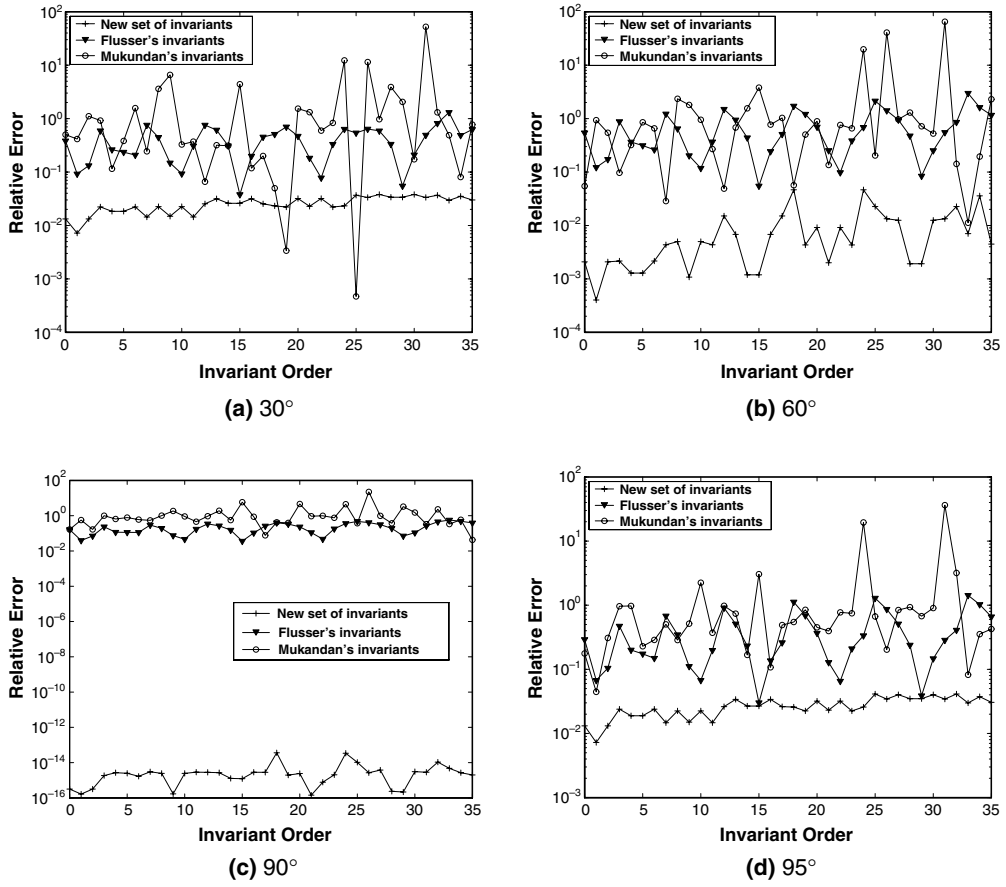

Fig. 3. Relative error against rotation, for the Mukundan's, Flusser's and the new complete set of similarity invariants (logarithmic scale except for the third image).

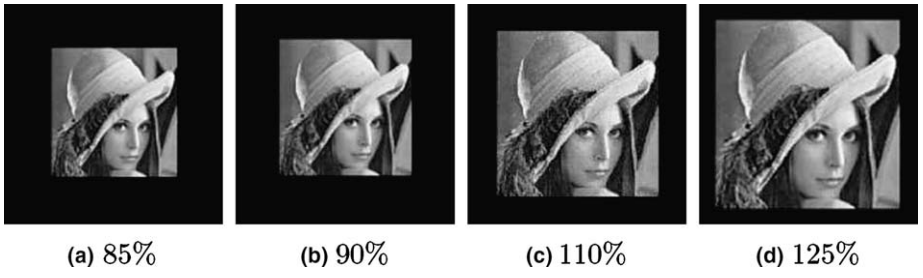

Fig. 4. Several scaled images of the original image.

corresponding to the new similarity invariant family seem to be smoother with respect to the order.

4. Image reconstruction from complex moments

In Section 2, we have seen that it is possible to recover the complex moments of an image from the complete set of invariants by mean of Eq. (7). We are now interested in the second step which consists in reconstructing the original image from its complex moments.

This inverse problem is known to be difficult in the case of non orthogonal moments, such as geometric and complex moments. The technic called "moment matching" by Teague (1980) is based upon creating a continuous function which moments match exactly the moments of the original function, through order $N_{\max}$. However, the method is impractical as it requires the solution to an increasing number of coupled equations, when higher order moments are considered (Prokop and Reeves, 1992). In this section, we propose an original method which consists in recovering the Fourier transform of an image from its complex moments. Then, the inverse Fourier transform is used to recover the original image.

4.1. Principle

The DFT $F(u,v)$ of an image can be expressed in terms of its complex moments according to (see Appendix B):

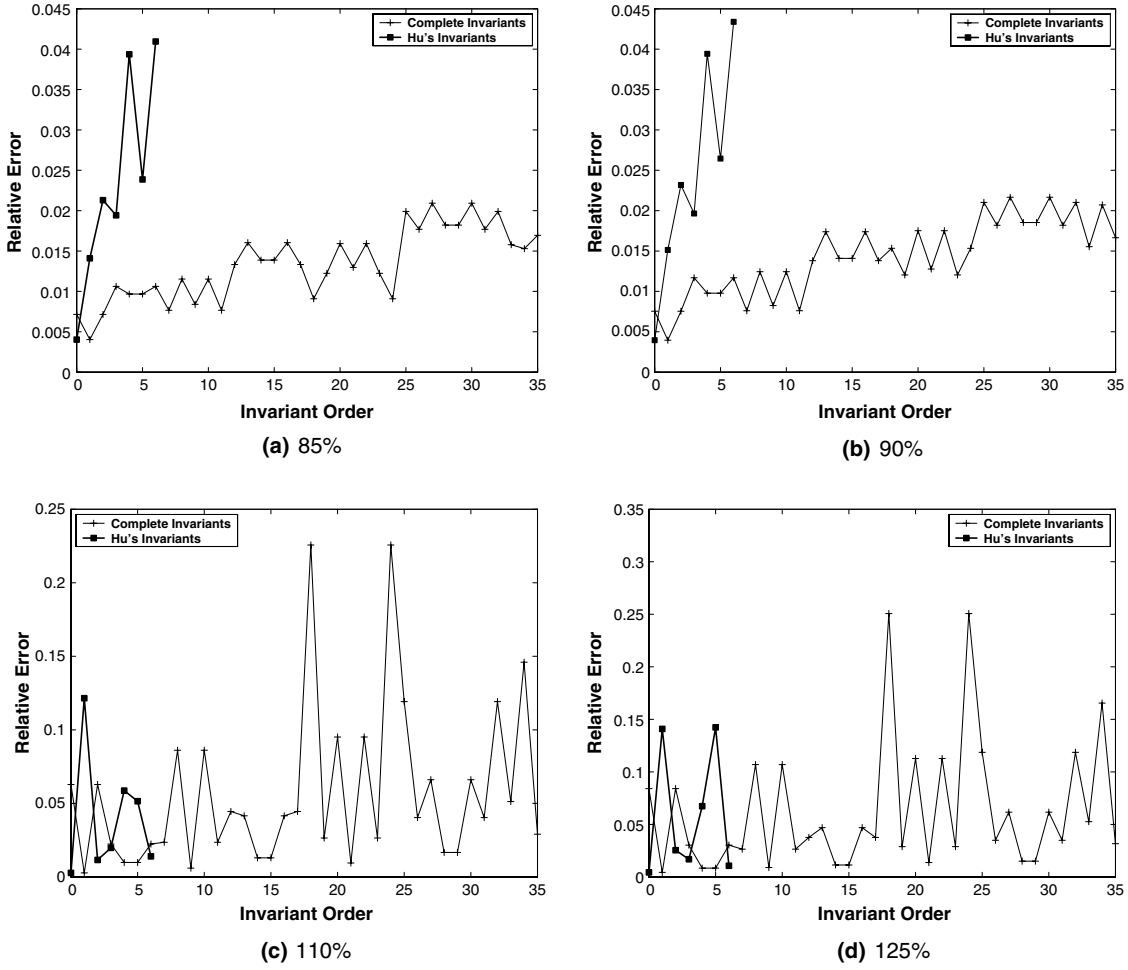

Fig. 5. Relative error against scale, for Hu's and new complete set of similarity invariants (linear scale).

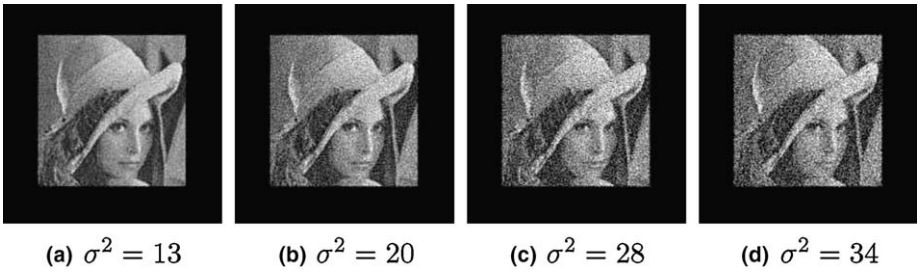

Fig. 6. Several noisy images of Lena.

$$F(u,v) = \sum_{p=0}^{\infty} \frac{(-\mathrm{i}\pi)^p}{p!} \sum_{k=0}^{p} \binom{p}{k} \left(\frac{u+\mathrm{i}v}{N}\right)^{p-k} \left(\frac{u-\mathrm{i}v}{M}\right)^{k} \times c_f(k,p-k). \quad (10)$$

To be computed, each Fourier harmonic needs all geometric moments which is not realistic from a computational point of view. However, we will see latter in experiments that only a limited number of moments has a real contribution in computation. The image function can then be recovered by computing the inverse DFT, according to

$$f(x,y) = \frac{1}{NM} \sum_{x=0}^{N-1} \sum_{y=0}^{M-1} F(u,v) \mathrm{e}^{2\mathrm{i}\pi\left(\frac{ux}{N}+\frac{vy}{M}\right)}.$$

4.2. Reconstruction error analysis

The normalized mean-square reconstruction error between a discrete image $f(n,m)$ of size $N \times M$ and its reconstructed version $\tilde{f}(n,m)$ from a finite set of its moments (up to order $N_{\max}$) is defined as

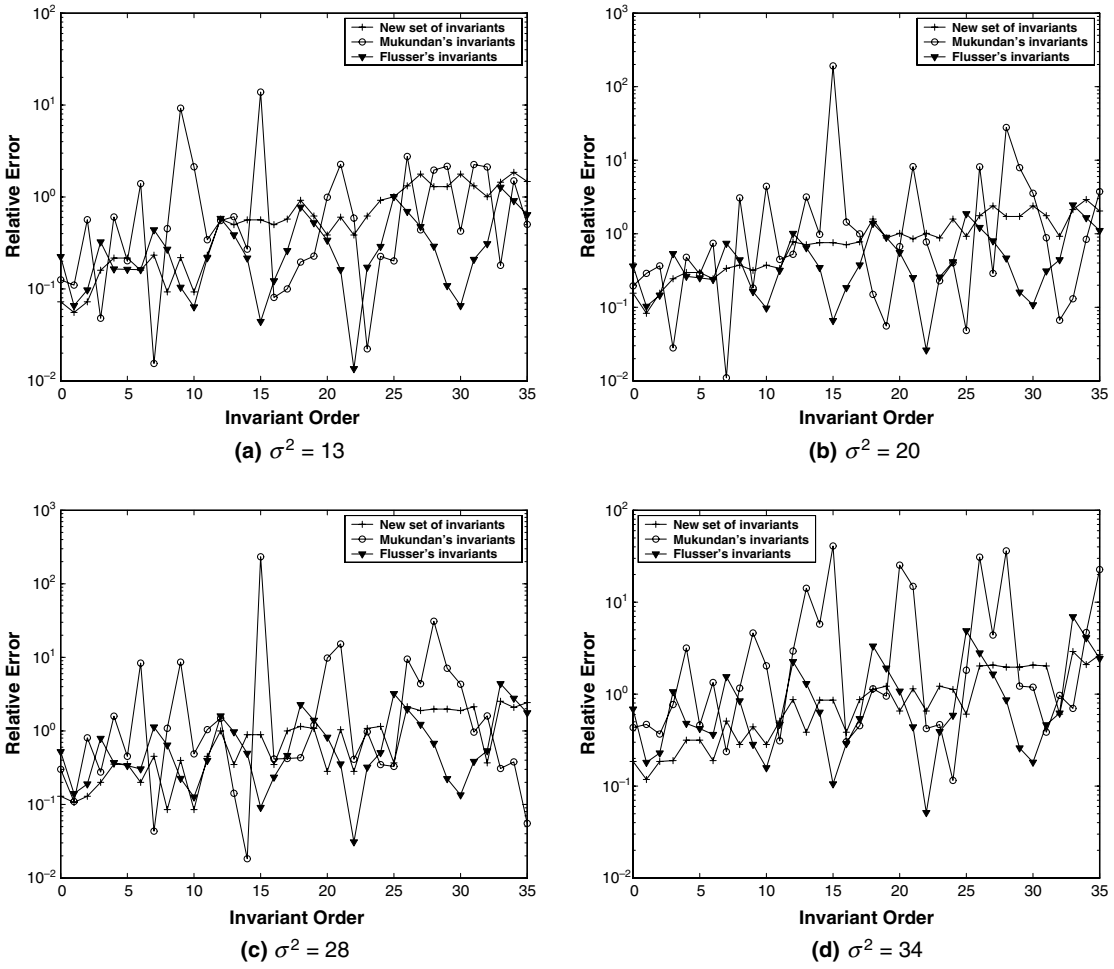

Fig. 7. Relative error against noise, for the Mukundan's, Flusser's and the new complete set of similarity invariants (logarithmic scale).

$$\bar{e}^2(N_{\max}) = \frac{\sum_{x=0}^{N-1}\sum_{y=0}^{M-1}[f(x,y) - \tilde{f}(x,y)]^2}{\sum_{x=0}^{N-1}\sum_{y=0}^{M-1}[f(x,y)]^2} \tag{11}$$

This error is considered as a good measure of the image representation and reconstruction ability of moments (Liao and Pawlak, 1996).

Up to a given order $N_{\max}$, Eq. (10) can be expressed in the form

$$F_{N_{\max}}(u,v) = \sum_{p=0}^{N_{\max}} \frac{(-i\pi)^p}{p!} \sum_{k=0}^{p} \binom{p}{k} \left(\frac{u+iv}{N}\right)^{p-k} \left(\frac{u-iv}{M}\right)^{k} \times c_f(k, p-k).$$

It is worth noting that as $N_{\max}$ approaches infinity, the reconstructed function $f_{N_{\max}}(x,y)$, computed from $F_{N_{\max}}(u,v)$, approaches the original function $f(x,y)$, i.e., more moments furnishes a higher quality reconstruction. This is illustrated in Fig. 8 which shows a general improvement in the quality of the basic and threshold reconstructed images when the order of moments increases.

In addition, we can see in the difference images that the number of mid-gray value pixels increases (correct reconstruction), whereas the number of black and white pixels decreases (incorrect pixels), as the reconstruction order increases. The normalized reconstruction error shown in Fig. 9 confirms this first remark.

The second remark is that a relatively small set of moments may characterize an image adequately. In fact, the letter 'E' is recognizable up to and including order 60, but fine details (high frequencies) can only be recreated by including higher order moments. To investigate the relation between higher order moments and higher Fourier frequencies in more depth, we have plotted the module values of some recovered DFT harmonics versus the order of moments used in reconstruction (Fig. 10). It is clear from this figure that higher frequencies need higher-order moments to be well approximated and a relatively small number of moments takes part in each harmonic (this number increases as the frequency increases).

Results in Table 1 confirm this remark. Indeed, we can observe that the higher order $N_{\max}$ needed to get $F_{N_{\max}}(u,v) \simeq F(u,v)$ with $F(u,v)$ computed directly from the original image, increases as the frequency also increases. Indeed, $F_{N_{\max}}(0,0)$ reaches $F(0,0)$ since the first order ($F(0,0) = C(0,0)$), whereas DFT coefficients of higher order $F_{N_{\max}}(1,1)$, $F_{N_{\max}}(2,1)$, $F_{N_{\max}}(2,3)$ and $F_{N_{\max}}(4,2)$

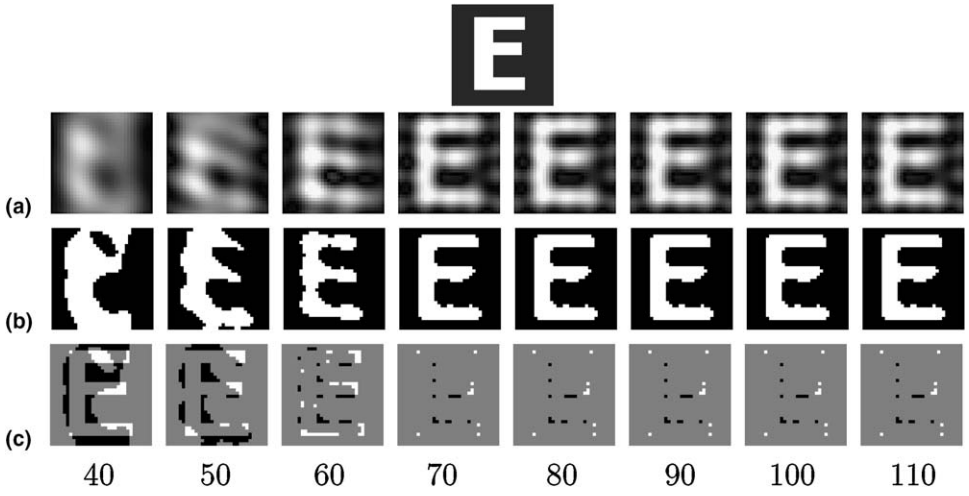

Fig. 8. Row (a) shows the reconstruction of a 32×32 letter 'E' with an increasing number of moments. Row (b) shows the binarized reconstructed images, with a threshold set to 0.5. Row (c) shows a pixel-by-pixel difference image between the reconstructed and the original images.

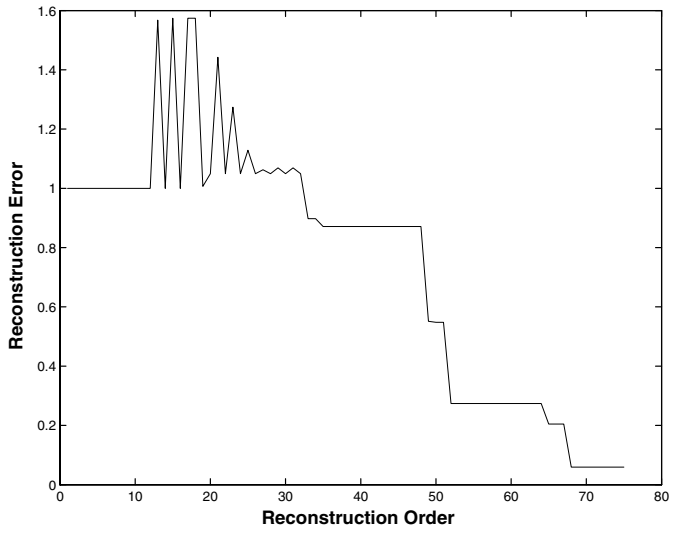

Fig. 9. Normalized mean-square reconstruction error of the 32×32 letter 'E' from complex moments (after binarization).

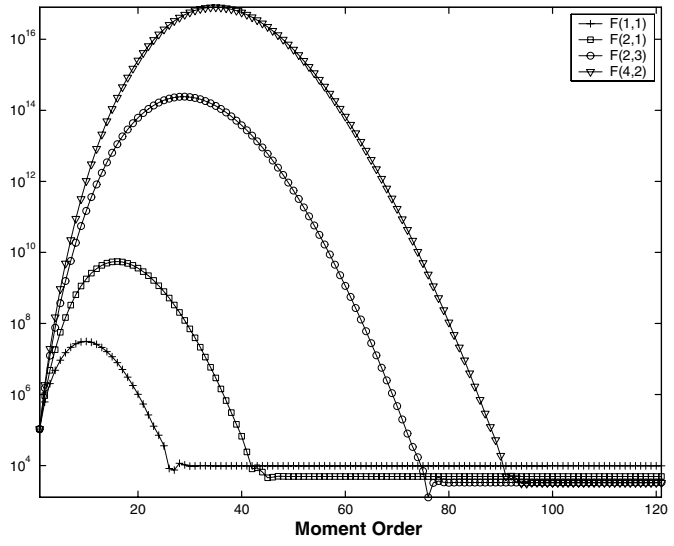

Fig. 10. Magnitude of complex moments used to reconstruct harmonics $F(1,1)$, $F(2,1)$, $F(2,3)$ and $F(4,2)$.

reach the expected value when $N_{\max} = 39$, 53, 87 and 107, respectively.

5. Conclusion

In this paper, we have presented a solution for the inverse problem from complex moments. Indeed, from the complete set of similarity invariants given by Eq. (5), an image can be recovered by reconstructing, first its complex moments using Eq. (7), and second, its DFT using Eq. (10).

Experiments on numerical invariancy confirm the robustness of the set and its interesting behavior with respect to Flusser and Suk's (2003), Mukundan's (2004) families of translation and rotation invariants. The additional scale invariance makes the complete family more general than the two others. Regarding image reconstruction, the proposed method seems to be effective and allow to recover the fine details of an image by including higher and higher order moments in the reconstruction process. One advantage of the method with respect to the "moment

Table 1
Order $N_{\max}$ needed to get a nearly exact approximation of a DFT harmonic computed directly from the original image

Harmonic	Value	$N_{\max}$
$F(0,0)$	106105	0
$F(1,1)$	$-4382.5 + 8833.4i$	39
$F(2,1)$	$-4758.3 - 1308.2i$	53
$F(2,3)$	$2187.3 - 1839.7i$	87
$F(4,2)$	$89.901 + 3252.8i$	107

matching'' strategy presented in (Teague, 1980) is that there is no coupled equations to solve.

As a perspective for further work, we may mention the application of the invariant family to the indexing of images into large databases. In addition, we will try to propose an extension of the descriptors to 3D shapes, since we know that the recognition of 3D objects independently of its size, position and orientation is an important and difficult problem in scene analysis.

Appendix A. Hu's invariants

Ming-Kuel (1962) defined seven descriptors, computed from non-linear combinations of normalized and centered geometric moments ($\eta_{p,q}$) through order $p+q=3$. All of them are invariant to object scale, position and orientation:

$$
\begin{aligned}
H_1 &= \eta_{2,0}+\eta_{0,2}\\
H_2 &= (\eta_{2,0}-\eta_{0,2})^2+4\eta_{1,1}^2\\
H_3 &= (\eta_{3,0}-3\eta_{1,2})^2+(3\eta_{2,1}-\eta_{0,3})^2\\
H_4 &= (\eta_{3,0}+\eta_{1,2})^2+(\eta_{2,1}-\eta_{0,3})^2\\
H_5 &= (\eta_{3,0}-3\eta_{1,2})+(\eta_{3,0}+\eta_{1,2})*((\eta_{3,0}+\eta_{1,2})^2-3(\eta_{2,1}+\eta_{0,3})^2)\\
&\quad +(3\eta_{2,1}+\eta_{0,3})*(\eta_{2,1}+\eta_{0,3})*(3(\eta_{3,0}+\eta_{1,2})^2-(\eta_{2,1}+\eta_{0,3})^2)\\
H_6 &= (\eta_{2,0}-\eta_{0,2})*((\eta_{3,0}+\eta_{1,2})^2-(\eta_{2,1}+\eta_{0,3})^2)\\
&\quad +4\eta_{1,1}*(\eta_{3,0}+\eta_{1,2})*(\eta_{2,1}+\eta_{0,3})\\
H_7 &= (3\eta_{2,1}-\eta_{0,3})(\eta_{3,0}+\eta_{1,2})*((\eta_{3,0}+\eta_{1,2})^2\\
&\quad -3(\eta_{2,1}+\eta_{0,3})^2)-(\eta_{3,0}-3\eta_{1,2})(\eta_{2,1}+\eta_{0,3})\\
&\quad *(3(\eta_{3,0}+\eta_{1,2})^2-(\eta_{2,1}+\eta_{0,3})^2)
\end{aligned}
$$

Appendix B. Relation between the complex moments and the Fourier transform of an image

Consider the Fourier transform $F(u,v)$ of the image function $f(x,y)$

$$F(u,v)=\iint_{\mathbb{R}^2} f(x,y)\mathrm{e}^{-2\mathrm{i}\pi(ux+vy)}\mathrm{d}x\,\mathrm{d}y.$$

By expanding the exponential function as a power series, we obtain

$$F(u,v)=\iint_{\mathbb{R}^2} f(x,y)\sum_{p=0}^{\infty}\frac{(-2\mathrm{i}\pi)^p}{p!}(ux+vy)^p\mathrm{d}x\,\mathrm{d}y.$$

If we interchange the order of summation and integration, we obtain

$$F(u,v)=\sum_{p=0}^{\infty}\frac{(-\mathrm{i}\pi)^p}{p!}\iint_{\mathbb{R}^2} f(x,y)(2(ux+vy))^p\mathrm{d}x\,\mathrm{d}y. \tag{B.1}$$

The expansion of $(ux+vy)^p$ according to Newton's binomial formula reveals the monomial product $x^k y^{p-k}$, which represents the kernel function of geometric moments, and consequently, results in a relation between geometric moments and the Fourier transform. As we are looking for a relationship between complex moments and the Fourier transform, we have to introduce in this expansion the complex monomial product $(x+\mathrm{i}y)^m(x-\mathrm{i}y)^n$, which represents the kernel function of complex moments. In addition, we can write

$$2(ux+vy)=(u+\mathrm{i}v)(x-\mathrm{i}y)+(u-\mathrm{i}v)(x+\mathrm{i}y). \tag{B.2}$$

By substituting Eq. (B.2) into (B.1), we obtain

$$
\begin{aligned}
F(u,v)=\sum_{p=0}^{\infty}\frac{(-\mathrm{i}\pi)^p}{p!}\iint_{\mathbb{R}^2} f(x,y)[&(u+\mathrm{i}v)(x-\mathrm{i}y)\\
&+(u-\mathrm{i}v)(x+\mathrm{i}y)]^p\mathrm{d}x\,\mathrm{d}y,
\end{aligned}
$$

and using Newton's binomial, we get

$$
\begin{aligned}
F(u,v)=\sum_{p=0}^{\infty}\frac{(-\mathrm{i}\pi)^p}{p!}\iint_{\mathbb{R}^2} f(x,y)&\sum_{k=0}^{p}\binom{p}{k}\\
&\times[(u+\mathrm{i}v)(x-\mathrm{i}y)]^{p-k}[(u-\mathrm{i}v)(x+\mathrm{i}y)]^k\mathrm{d}x\,\mathrm{d}y.
\end{aligned}
$$

Then, if we interchange the order of summation and integration, we obtain

$$
\begin{aligned}
F(u,v)&=\sum_{p=0}^{\infty}\frac{(-\mathrm{i}\pi)^p}{p!}\sum_{k=0}^{p}\binom{p}{k}(u+\mathrm{i}v)^{p-k}(u-\mathrm{i}v)^k\\
&\quad\times\iint_{\mathbb{R}^2} f(x,y)(x-\mathrm{i}y)^{p-k}(x+\mathrm{i}y)^k\mathrm{d}x\,\mathrm{d}y,\\
&=\sum_{p=0}^{\infty}\frac{(-\mathrm{i}\pi)^p}{p!}\sum_{k=0}^{p}\binom{p}{k}(u+\mathrm{i}v)^{p-k}(u-\mathrm{i}v)^k c_f(k,p-k).
\end{aligned}
$$

In a similar way, we can easily show that the DFT and the complex moments are related according to

$$F(u,v)=\sum_{p=0}^{\infty}\frac{(-\mathrm{i}\pi)^p}{p!}\sum_{k=0}^{p}\binom{p}{k}\left(\frac{u+\mathrm{i}v}{N}\right)^{p-k}\left(\frac{u-\mathrm{i}v}{M}\right)^k c_f(k,p-k).$$

References

Abu-Mostafa, Y.S., Psaltis, D., 1984. Recognitive aspects of moments invariants. IEEE Trans. Pattern Anal. Mach. Intell. 6 (6), 698–706.

Abu-Mostafa, Y.S., Psaltis, D., 1985. Image normalization by complex moments. IEEE Trans. Pattern Anal. Mach. Intell. 7 (1), 46–55.

Balslev, I., 1998. Noise tolerance of moments invariant in pattern recognition. Pattern Recognit. Lett. 19, 1183–1189.

Crimmins, T.R., 1982. A complete set of Fourier descriptors for two dimensional shape. IEEE Trans. Syst. Man Cybernet. 121 (6), 848–855.

Davis, P.J., 1977. Plane regions determined by complex moments. J. Approx. Theory 19, 148–153.

Derrode, S., Ghorbel, F., 2001. Robust and efficient Fourier–Merlin transform approximations for invariant grey-level image description and reconstruction. Comput. Vis. Image Understand. 83 (1), 57–78.

Derrode, S., Mezhoud, R., Ghorbel, F., 2000. Comparison between two complete sets of shape descriptors for 2D gray-level object content-based retrieval. Ann. Telecommun. 55 (3/4), 184–193, in french. URL http://www.fresnel.fr/perso/derrode/index.html.

Flusser, J., 2002. On the inverse problem of rotation moment invariants. Pattern Recognit. 35, 3015–3017.

Flusser, J., Suk, T., 2003. Construction of complete and independent systems of rotation moment invariants. In: Petkov, N., Westenberg, M.A. (Eds.), Proc. of the Computer Analysis of Images and Patterns Conf., Lecture Notes in Computer Science, vol. 2756. Springer, Berlin, pp. 41–48.

Flusser, J., Suk, T., Saic, S., 1996. Recognition of blurred images by the method of moments. IEEE Trans. Image Process. 5 (3), 533–538.

Ghorbel, F., 1994. A complete invariant description for gray-level images by the harmonic analysis approach. Pattern Recognit. Lett. 15, 1043–1051.

Khotanzad, A., Hong, Y.H., 1990. Invariant image recognition by Zernike moments. IEEE Trans. Pattern Anal. Mach. Intell. 12 (5), 489–497.

Liao, S.X., Pawlak, M., 1996. On image analysis by moments. IEEE Trans. Pattern Anal. Mach. Intell. 18 (3), 254–266.

Liu, J., Zhang, T., 2005. Recognition of the blurred image by complex moment invariants. Pattern Recognit. Lett. 26 (8), 1128–1138.

Ming-Kuel, H., 1962. Visual pattern recognition by moment invariants. IRE Trans. Inf. Theory, 179–187.

Mukundan, R. 2004. A new class of rotational invariants using discrete orthogonal moments. In: Proc. of the 6th IASTED Int. Conf. on Signal and Image Proc. (SIP'04), Honolulu, Hawaii (USA), pp. 80–84.

Mukundan, R., Ong, S.H., Lee, P.A., 2001. Image analysis by Tchebichef moments. IEEE Trans Image Process. 10 (9), 1357–1364.

Prokop, R.J., Reeves, A.P., 1992. A survey of moment-based techniques for unoccluded object representation and recognition. Graphical Models Image Process. 54 (5), 438–460.

Ren, H., Ping, Z., Bo, W., Wu, W., Sheng, Y., 2003. Multidistortion-invariant image recognition with radial harmonic Fourier moments. J. Opt. Soc. Am. A 20 (4), 631–637.

Sheng, Y.L., Shen, L.X., 1994. Orthogonal Fourier–Merlin moments for invariant pattern recognition. J. Opt. Soc. Am. A 11, 1748–1757.

Suk, T., Flusser, J., 2003. Combined blur and affine moment invariants and their use in pattern recognition. Pattern Recognit. 36, 2895–2907.

Suk, T., Flusser, J., 2004. Projective moment invariants. IEEE Trans. Pattern Anal. Mach. Intell. 26 (10), 1364–1367.

Suk, T., Flusser, J. 2004. Graph method for generating affine moment invariants. In: Proc. of the 17th Int. Conf. on Pattern Recognit. (ICPR'04), vol. 2, Cambridge, UK, pp. 192–195.

Teague, M.R., 1980. Image analysis via the general theory of moments. J. Opt. Soc. Am. A 70 (8), 920–930.

Wong, W.H., Siu, W.C., Lam, K.M., 1995. Generation of moment invariants and their uses for character recognition. Pattern Recognit. Lett. 16, 115–123.

Yap, P.T., Paramersan, R., Ong, S.H., 2003. Image analysis by Krawtchouk moments. IEEE Trans. Image Process. 12 (11), 1367–1377.